Effects of configurational, positional and vibrational degrees of freedom on an alloy phase diagram: a Monte Carlo study of $Ga_{1-x}In_xP$

Effects of configurational, positional and vibrational degrees of freedom on an alloy phase diagram: a Monte Carlo study of $Ga_{1-x}In_xP$

A Silverman†‡, Alex Zunger§, R Kalish†‡ and Joan Adler†

† Physics Department, Technion—Israel Institute of Technology, Haifa, Israel 32000
‡ Solid State Institute, Technion—Israel Institute of Technology, Haifa, Israel 32000
§ National Renewable Energy Laboratory, Golden, Colorado, 80401

Abstract. A large number of *ab initio* calculated total energies of different GaP/InP superlattices are used to fit a Born–Oppenheimer energy surface. Monte Carlo simulations are then performed on this surface, including treatment of configurational, positional and vibrational degrees of freedom. This permits isolation of the effects of these degrees of freedom on the thermodynamic behaviour. We find the following.

(i) Positional relaxation of the atoms to equilibrium, (off-site) locations lowers enormously both the mixing enthalpy (by ∼ 50%) and the miscibility gap (MG) temperature (from $T_{MG} = 1746$ K to $T_{MG} = 833$ K).

(ii) Allowance for configurational correlations (absent in a mean-field treatment) reduces both the entropy and the enthalpy, leading to a net *increase* of ∼ 70 K in T_{MG}.

(iii) Vibrations *reduce* T_{MG} by ∼ 30 K leading to a final $T_{MG} = 870$ K. The calculated phase diagram is in accord with experiment.

1. Introduction

The thermodynamics of alloys reflects the interplay of configurational, positional, vibrational and electronic degrees of freedom [1]. *Configurational* degrees of freedom refer to the many ways that atoms can be arranged on a static, non-vibrating lattice in its electronic ground state. These degrees of freedom are conveniently labelled by pseudo spin variables $\hat{S}_i$. In binary $A_{1-x}B_x$ systems these take the values $+1$ or -1 if lattice site i is occupied by atom A or atom B, respectively. The collection $\{\hat{S}_i\}$ for $i = 1 \ldots N$ sites defines any one of the 2^N possible (ordered or disordered) configurations σ on a binary lattice with N sites. In each configuration σ, the N atoms can be displaced by amounts $\{R_i\}$ from their 'ideal', unrelaxed lattice positions. Such static *positional* relaxations, often induced by size differences between the atoms, always lower the internal energy. A Born–Oppenheimer internal energy surface of an alloy, $E_{direct}[\{\hat{S}_i\}; \{\tau\}; \{R_i\}]$ can thus be parametrized in terms of its configurational degrees of freedom $\{\hat{S}_i\}$ as well as its positional cell-internal $\{R_i\}$ and cell-external $\{\tau\}$ variables. Knowledge of this surface and its spatial derivatives provides the *vibrational* degrees of freedom. Unlike static relaxations, the ensuing dynamic lattice vibrations are manifested by atomic displacements towards directions that do not necessarily lower the internal energy. In the absence of electronic excitations connecting different Born–Oppenheimer surfaces [2], knowledge of $E_{direct}[\{\hat{S}_i\}; \{\tau\}; \{R_i\}]$ thus defines the problem of alloy energetics. In practice, this energy surface is obtained either from *ab initio* total energy

calculations [3] or from parametrized effective potentials [4, 5, 6, 8]. Both approaches are termed here as 'direct calculations'. In this paper we will consider insulating alloys (i.e. no electronic excitations) and discuss the effects of configurational, positional and vibrational degrees of freedom on the temperature-composition phase diagram. We will introduce a general approach that permits a separation between static and dynamic effects, and illustrate this approach in application to the phase-diagram of the $(GaP)_{1-x}(InP)_x$ semiconductor alloy. We show dramatic changes introduced by static positional relaxations and smaller effects due to dynamic vibrations.

2. Method of calculation

2.1. General discussion

Previous approaches that treat configurational and positional degrees of freedom can be divided into 'direct methods' which apply statistical mechanics techniques directly to the Born–Oppenheimer surface $E_{direct}[\{\hat{S}_i\}; \{\tau\}; \{R_i\}]$, and 'cluster expansion' methods which utilize a generalized Ising description in which atomic displacements do not appear explicitly. These approaches are illustrated schematically in figure 1. We now briefly describe the guiding principles of these methods. The cluster expansion (CE) [1, 9] consists
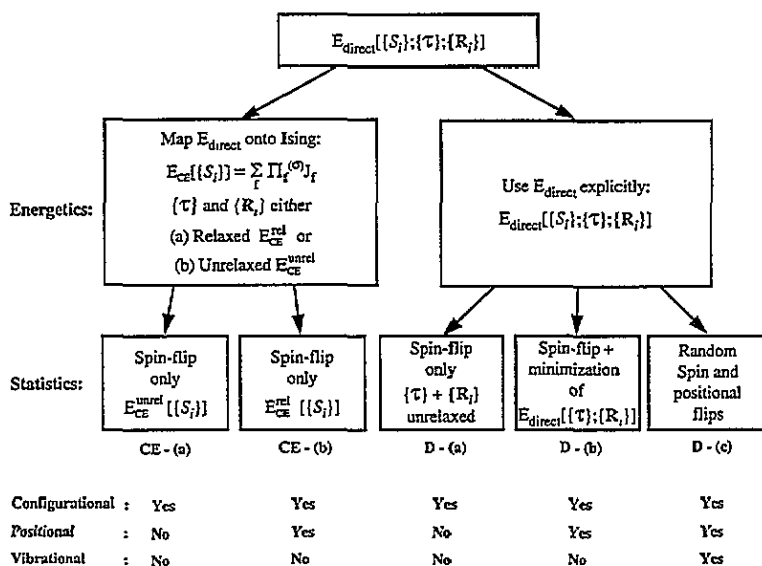

Figure 1. Schematic illustration of the different approaches for the calculations of the $x - T$ phase diagram. See text for explanation.

of mapping the set $\{E_{direct}(\sigma)\}$ of directly calculated total energies onto an Ising-like series. In fact, for a lattice with N sites, the problem of finding the energies of the 2^N possible configurations can be *exactly* [10] mapped onto the Hamiltonian

$$E_{CE}(\sigma) = J_0 + \sum_i J_i \hat{S}_i(\sigma) + \sum_{j<i} J_{ij} \hat{S}_i(\sigma)\hat{S}_j(\sigma) + \sum_{k<j<i} J_{ijk} \hat{S}_i(\sigma)\hat{S}_j(\sigma)\hat{S}_k(\sigma) + \dots \quad (1)$$

for configuration σ, where the J's are 'interaction energies', and the first summation is over all sites (i) in the lattice, the second over all pairs of sites (ij), the third over all triplets

(ijk), and so on. These constitute the basic 'figures' of the lattice. The interaction energies, $\{J\}$, are the same for all configurations σ. The Hamiltonian of equation (1) contains 2^N interaction energies J, which are used to describe the energies of the 2^N configurations σ. Consequently, equation (1) can be viewed as defining a set of linear equations, in which $2^N \times 2^N$ matrix of pseudo-spin products multiplies a 2^N vector of J's, giving a vector of the energies of the 2^N configurations. The practical utility of the CE rests on the fact that the interaction energies $\{J\}$ can be calculated using only *partial information* on $E_{\text{direct}}[\{\hat{S}_i\}; \{\tau\}; \{R_i\}]$ [1, 11] and that in many cases only a small number of $\{J\}$ ($\ll 2^N$) turn out to be numerically important [1]. Thus, if these important J's are known, the energy $E_{\text{CE}}(\sigma)$ of any of the 2^N configurations can be calculated almost immediately by simply calculating the spin products and summing equation (1). Because the Ising representation of the energy can be calculated rapidly, and is also a linear function of the spin products, one can readily (i) apply linear programming techniques to find ground state structures (e.g., [12]), (ii) use statistical mechanics techniques such as the cluster variation method [13] or Monte Carlo [14] to calculate phase diagrams, and (iii) calculate the energy of an arbitrarily complex configuration [15]. A direct calculation of configurational and spin depended excess energies of simulated samples using equation (1) is much easier than repeated quantum mechanical calculations.

When the interaction energies $\{J\}$ are calculated from E_{direct} [1, 11], one can use either relaxed or unrelaxed atomic geometries, thus finding the corresponding relaxed or unrelaxed sets, $\{J_{\text{unrel}}\}$ or $\{J_{\text{rel}}\}$. These two possibilities are denoted as CE-(a) and CE-(b) in figure 1. This choice is possible since the relaxed geometry for configuration σ is a unique function of the unrelaxed geometry of σ. Most statistical mechanical descriptions of 'chemical alloys' $A_{1-x}B_x$ or 'magnetic alloys' belong to type CE-(a) disregarding the positional degrees of freedom $\{R_i\}$, and focusing only on the configurational degrees of freedom $\{\hat{S}_i\}$. (The spins can be scalar Ising spins, or vector ones, and in some cases a combination [16].) These standard CE-(a) models (figure 1) are reviewed, e.g. [9, 17]. The underlying assumption of unrelaxed CE-(a) models is that the atomic positions are invariant under changes in site occupations. Specifically, that the *energy* of a particular configuration is not affected much by the relaxation of the atoms off their ideal lattice sites. This assumption appears to be physically unreasonable for alloys made of *size-mismatched constituents* A and B: the atomic positions $\{R_i\}$ of a structure with a small atom surrounded by large atoms must be different from that of a large atom surrounded by large atoms, etc. Cluster expansions that include relaxation (denoted CE-(b) in figure 1) have recently been applied to transition metal alloys [1, 2, 18, 19, 20] and to semiconductor alloys [21, 22, 23, 24, 25].

In 'direct (D) methods' one avoids series expansion (thus, series truncation) of E_{direct}. Instead, one couples the energy functional directly to a statistical mechanical lattice treatment, e.g., Monte Carlo simulation [5, 6, 8]. Here, three principal choices exist, denoted in figure 1 as D-(a), D-(b) and D-(c).

In the first level D-(a), one assumes that all atoms are located on the nominal lattice sites irrespective of the atomic configuration. In this case one samples in $E_{\text{direct}}[\{\hat{S}_i\}]$ only the configurational (spin) degrees of freedom during the statistical simulation. This D-(a) (direct, unrelaxed, static) approach thus neglects both positional and vibrational degrees of freedom and is analogous to approach CE-(a) in the context of Ising expansions. Most direct-functional Monte Carlo simulations of alloys belong to this category [17, 26].

In the second [D-(b)] level, one minimizes $E_{\text{direct}}[\{\tau\}; \{R_i\}]$ with respect to $\{\tau\}$ and $\{R_i\}$ at each spin-configuration $\{\hat{S}_i\}$ encountered in the statistical simulation. Here the atomic positions $\{R_i\}$ are thus obtained *deterministically* for each spin configuration since one is following a *minimum energy* path. This D-(b) (direct, relaxed, static) approach includes

configurational and positional effects but, since only deterministic, energy-lowering atomic displacements are sought, dynamic vibrational effects are neglected. Thus it is analogous to CE-(b) in the context of cluster expansion.

Finally, in the third (D-(c)) level, one treats configurational and positional degrees of freedom on *equal footing*, e.g. by selecting *random* configurational changes $\{\hat{S}_i\}$ and *random* displacements $\{\Delta R_i\}$ during the statistical simulation. This D-(c) (direct, relaxed, dynamic) approach includes configurational, positional and vibrational effects.

Given a convenient Born–Oppenheimer surface E_{direct} one can either parametrize it in terms of a cluster expansion (equation (1)) and apply methods CE-(a) and CE-(b) or directly apply methods D-(a), D-(b) and D-(c), in conjunction with Monte Carlo simulations. The direct approach allows comparing the phase diagram in step (a), (b), and (c) and thus isolating the effects of the different degrees of freedom. While it is interesting to inquire as to how well cluster expansions mimic the direct approaches (e.g., CE-(a) *versus* D-(a) or CE-(b) *vs* D-(b)), here we focus on the more accurate (but computationally more extensive) direct methods.

In what follows we will describe the construction of an approximate but rather accurate Born–Oppenheimer surface E_{direct} $[\{\hat{S}_i\}; \{\tau\}; \{R_i\}]$ for the $(GaP)_{1-x}(InP)_x$ FCC alloy (section 2.2) and describe how Monte Carlo simulations are carried out using approaches D-(a), D-(b) and D-(c) (section 2.3). Results are provided in section 3 while a summary is given in section 4.

2.2. Parametrizing an energy surface for $(GaP)_{1-x}(InP)_x$

The Born–Oppenheimer energy $E_{\text{direct}}(\sigma)$ is modelled here by the valence force field (VFF) of Keating [27] (see also [28, 29]):

$$E_{\text{direct}}(\sigma) = \sum_l \sum_{m=1}^{4} \frac{3}{8d_{AC}^2} \alpha_{AC}[r_m(l, 1) \cdot r_m(l, 1) - d_{AC}^2]^2$$

$$+ \sum_l \sum_{s=1}^{2} \sum_{m=1}^{3} \sum_{n=m+1}^{4} \frac{3}{8d_{AC}^2} \beta_{A-C-A}\left[r_m(l, s) \cdot r_n(l, s) + \frac{d_{AC}^2}{3}\right]^2 \quad (2)$$

where $d_{AC} = R_{ij}^0$ is the equilibrium interatomic distance in the binary constituents, $r_m(l, s)$ is the vector connecting atom s in unit cell l to its mth nearest neighbour, and α_{AC} and $\beta_{A--C--A}$ are the bond stretching and bond bending force constants. Martin [29] calculated the values of α and β of equation (2.2) for *binary* AC and BC materials. Since this VFF correctly describes the elastic coefficients, lattice constants, bulk moduli and phonons of the binary compounds InP and GaP, we leave the *binary* β's and α's unchanged. For the *ternary* $A_xB_{1-x}C$ compound, Martin [29] suggested the relations

$$\beta_{A-C-A} = \beta_{C-A-C}$$
$$\beta_{B-C-B} = \beta_{C-B-C}$$
$$\beta_{A-C-B} = \frac{1}{2}(\beta_{A-C-A} + \beta_{B-C-B}). \quad (3)$$

Generalizing this, we can introduce individual bond bending parameters for the ternary alloy, namely β_{A-C-A}, β_{C-A-C}, β_{B-C-B}, β_{C-B-C}, and β_{A-C-B}. Figure 2 illustrates these parameters for A=In, B=Ga, and C=P. We can write that in parametric form as

$$\beta_{P-In-P} = (1 + f_{In})\beta'_{In-P-In}$$
$$\beta_{In-P-In} = (1 - f_{In})\beta'_{In-P-In}$$

$$\beta_{Ga-P-Ga} = (1 + f_{Ga})\beta'_{Ga-P-Ga}$$
$$\beta_{P-Ga-P} = (1 - f_{Ga})\beta'_{Ga-P-Ga} \qquad (4)$$

where β'_{A-C-A} are the VFF binary bond bending parameters. Note that the In–P–Ga bond angle does not occur in binary compounds. It is easy to verify from equation (2.4) that using the binary β_{A-C-A}, and β_{B-C-B}, and the three new parameters $\{\beta_{In-P-Ga}, f_{In}, f_{Ga}\}$ does not change the VFF elastic constants for the binary compounds. The ternary force

Table 1. Formation enthalpies ΔH for ordered structures of InP/GaP, where A=GaP and B=InP. The structures are described as $(AC)_p(BC)_q$ superlattices with layer repeats (p, q) and orientation G. The formation enthalpies were calculated using LDA, the original Keating VFF potential (VFF) [27, 29], and our ternary potential (T-VFF). The units are meV/four-atoms, and the symbols define structure names (as defined in [30]).

Formula	Source	Orientation					Row average deviations[a]
		[111]	[001]	[110]	[201]	[113]	
		CP	CA	CA	CA	CP	
AB	LDA	144.2	90.3	90.3	90.3	144.2	
	T-VFF	132.4	93.5	93.5	93.5	132.4	6.6
	VFF	133.6	87.5	87.5	87.5	133.6	5.9
		$\alpha 1$	$\beta 1$	$\gamma 1$	$\gamma 1$	$\gamma 1$	
AB$_2$	LDA	128.0	81.9	46.6	46.6	46.6	
	T-VFF	127.4	90.8	43.6	43.6	43.6	5.0
	VFF	128.7	87.3	58.9	58.9	58.9	9.8
		$\alpha 2$	$\beta 2$	$\gamma 2$	$\gamma 2$	$\gamma 2$	
A$_2$B	LDA	126.7	79.1	45.6	45.6	45.6	
	T-VFF	109.1	77.2	45.7	45.7	45.7	5.0
	VFF	109.7	72.8	59.4	59.4	59.4	14.9
		V1	Z1	Y1	F1	W1	
AB$_3$	LDA	110.4	72.9	54.3	32.0	62.9	
	T-VFF	112.4	80.3	53.6	34.0	63.8	4.6
	VFF	113.5	78.0	60.8	43.6	72.0	10.9
		V2	Z2	Y2	CH	W2	
A$_2$B$_2$	LDA	141.8	90.6	60.7	29.8	61.0	
	T-VFF	132.1	94.1	60.2	40.2	62.4	6.0
	VFF	132.6	91.1	78.1	57.1	75.8	16.0
		V3	Z3	Y3	F3	W3	
A$_3$B	LDA	105.1	67.7	54.9	45.3	69.6	
	T-VFF	88.7	62.7	58.1	52.2	67.8	6.9
	VFF	89.1	59.4	64.1	61.0	74.7	13.2
Columns average deviations[b]:							
	T-VFF	9.7	5.0	1.8	4.3	3.2	
	VFF	9.4	4.7	10.3	13.9	11.0	

[a] The average deviations relative to the LDA values for the rows.
[b] The average deviations relative to the LDA values for the columns.

constants of equation (2.4) were fit to first-principle total energy calculations on ordered periodic structures [30]. Most of these structures can be described [15] as $(AC)_p/(BC)_q$ superlattices of periods (p, q) and direction $\hat{G}$ (table 1). Table 2 gives the two additional

structures which are not superlattices. The fully relaxed excess energies $\{\Delta E_{LDA}(s, V)\}$ of 25 ordered structures $\{s\}$ of the $(GaP)_p/(InP)_q$ compounds were calculated [30] in the local-density approximation (LDA) as implemented by the general-potential, linear augmented-plane-wave (LAPW) method [31]. (The calculations of [21] have been refined in [30] by adding more k-points, using better basis set convergence, and adding many more structures). Using equations (2.2) and (2.4) we have also calculated the excess energies of the ordered structures $\{\Delta E_{VFF}(s, V, \beta_{In-P-Ga}, f_{In}, f_{Ga})\}$. For each of the structures, the excess energy of the relaxed cell was calculated where the cell external coordinates (i.e. 3×3 matrix which describes the parallelepiped shaped unit cell) as well as the cell internal coordinates (i.e. the atomic coordinates tensor) were relaxed using a Monte Carlo algorithm at $T = 0$. To fit VFF to LDA we defined a cost function which expresses the difference between the VFF and LDA excess energies as a function of the three parameters $\beta_{In-P-Ga}$, f_{In}, and f_{Ga}

$$C(\beta_{In-P-Ga}, f_{In}, f_{Ga}) = \sum_{\substack{\text{ordered} \\ \text{structures}}} |\Delta E_{LDA}(s, V) - \Delta E_{VFF}(s, V, \beta_{In-P-Ga}, f_{In}, f_{Ga})|. \tag{5}$$

Table 2. Formation enthalpies ΔH for the two luzonite (L1 and L3) ordered structures of GaInP, where A=GaP and B=InP. The formation enthalpies were calculated using LDA, our ternary potential (T-VFF), and Keating original VFF potential (VFF). The units of the formation enthalpies are meV/four-atoms.

Formula	Name	Potential	ΔH
AB_3	L1	LDA	57.4
		T-VFF	60.7
		VFF	57.1
A_3B	L3	LDA	77.9
		T-VFF	81.8
		VFF	80.8

A simulated annealing algorithm [32] was used to find the values of the parameters which minimize $C(\beta_{In-P-Ga}, f_{In}, f_{Ga})$. The surface of the cost function $C(\beta_{In-P-Ga}, f_{In}, f_{Ga})$ is complex, having many *local* minima. In some cases, the simulated annealing algorithm reached minima with $|f_{In}| > 1$ or $|f_{Ga}| > 1$, resulting (see equation (2.4)) in unphysical *negative* values of one of the bond bending force constants β_{A-C-A}. We regard these local minima of $C(\beta_{In-P-Ga}, f_{In}, f_{Ga})$ as 'forbidden minima', so we add to the cost function a constraint function, multiplied by a Lagrange multiplier

$$C'(\beta_{In-P-Ga}, f_{In}, f_{Ga}) = C(\beta_{In-P-Ga}, f_{In}, f_{Ga}) + \lambda(h_{In} + h_{Ga}) \tag{6}$$

where h_A are the functions

$$h_A = \begin{cases} 0 & \text{if } -1 \leqslant f_A \leqslant 1 \\ 1 & \text{otherwise.} \end{cases} \tag{7}$$

In this way, the modified cost function C' is allowed to pass through the 'forbidden minima', but it is most probable that it will not stay there. The value of the Lagrange multiplier λ was chosen to be comparable to the depth of the valleys of C (~ 5 meV) as observed during test runs of the simulated annealing algorithm.

The best fit values for the parameters of equation (2.4) are

$$\beta_{In-P-Ga} = 1.6715 N/m,$$

$$f_{Ga} = -0.4621$$
$$f_{In} = 0.9705. \tag{8}$$

Note that the various structures included in the fit correspond to a significant range (± 0.3Å) of atomic displacements, thus, in so far as the LDA is accurate, we can use our parametrized surface for calculating vibrations. In all our calculations, each atom is fourfold coordinated. The resulting β values are given in the insert of figure 2. Since our VFF is fit also to
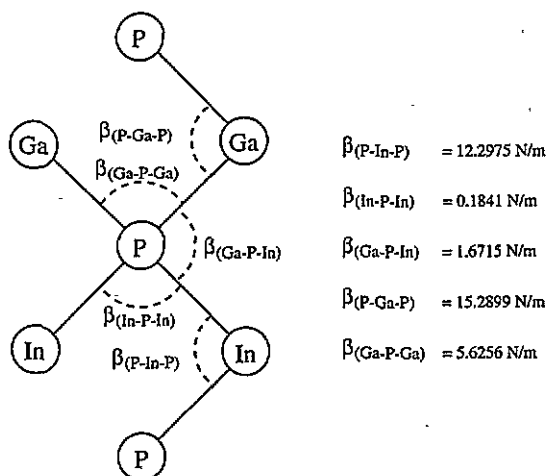

$\beta_{(P-In-P)}$ = 12.2975 N/m

$\beta_{(In-P-In)}$ = 0.1841 N/m

$\beta_{(Ga-P-In)}$ = 1.6715 N/m

$\beta_{(P-Ga-P)}$ = 15.2899 N/m

$\beta_{(Ga-P-Ga)}$ = 5.6256 N/m

Figure 2. Schematic diagram depicting the different bond bending force constants in the Ga$_{1-x}$In$_x$P random alloy. The five force constants β of the VFF potential are labeled. The best values found in our fit to the LAPW results are given.

ternary (T) data, we will refer to it as T-VFF, to be distinguished from the Keating-Martin binary VFF. Tables 1 and 2 compare the LDA values of $\Delta E(s, V_{eq})$ to the fitted T-VFF values. We see that the current T-VFF potential considerably improves the overall fit compared to the original VFF potential. This is particularly true for the superlattice structures in the orientations [110], [201], and [113], where the fit of the original VFF potential is quite poor. The fit of the original VFF potential for the superlattice structures in the orientations [111] and [001] and for the Luzonite structures (table 2) is very good; our new fit thus leaves these values essentially unchanged. The existence of a small RMS error over a wide range of compositions and superlattice orientations (tables 1 and 2) suggests that our T-VFF can also be used to predict energies $\Delta E(\hat{S}', Veq)$ of structure $\{\hat{S}'\}$ outside the set $\{\hat{S}\}$ used in the fit.

2.3. Phase diagram calculations

We will describe in what follows our most general procedure D-(c) (see figure 1) in which configurational, positional and vibrational degrees of freedom are retained. The simpler procedures D-(a) and D-(b) will then be described by eliminating a few steps from the more general approach D-(c):

(i) The initial spin configuration $\{\hat{S}_i\}$ is chosen so that the A/B sublattice is occupied randomly according to the alloy composition x. The initial atomic coordinates $\{R_i\}$ are

chosen as the zinc-blende positions $\{R_i^0\}$ of a cubic cell with periodic boundary conditions and a Vegard lattice constant $a(x)$.

(ii) The displacement field is defined as follows: first, atoms (indexed by i) are chosen randomly. Subsequently, three types of Monte Carlo displacements/flips are introduced: (a) At each step, a random and small coordinate displacement ΔR_i is chosen, and the new positions $\{R_i'\}$ are mapped : $\{R_i'\} \rightarrow \{R_i\} + \Delta R_i$. (b) About every $1/P_S$ steps the spin $\hat{S}_i$ is flipped so $\{\hat{S}_i\}$ is mapped to $\{\hat{S}_i'\}$. (c) About every $1/P_V$ steps a random small volume change ΔV is chosen and the volume of the cell is mapped by $\{R_i'\} \rightarrow \{R_i\} + \{\Delta R_i\}$, where $\Delta R_i = (1, 1, 1)\Delta V$ for all i. Hence, P_S and P_V are the probabilities of spin flip and volume change respectively. We chose $P_S = 0.05$ and $P_V = 1/N$ where N is the number of atoms in the sample. We found that these are optimum values for stability as well as fast convergence of the MC algorithm.

(iii) Each MC step is accepted with a probability P_{accept} where

$$P_{\text{accept}} = \begin{cases} \exp(\delta E)/k_B T) & \text{if } \delta E > 0 \\ 1 & \text{otherwise} \end{cases} \tag{9}$$

where T is the temperature of the sample, and k_B is the Boltzmann constant. The energy change due to spin and position changes is

$$\delta E = \Delta E_{\text{direct}}[\{\hat{S}_i'\}; \{R_i'\}] + \sum i \mu_i(\hat{S}_i') - \Delta E_{\text{direct}}[\{\hat{S}_i\}; \{R_i\}] - \sum_i \mu_i(\hat{S}_i). \tag{10}$$

Here, $\Delta E_{\text{direct}}[\{\hat{S}_i\}; \{R_i\}]$ is calculated from equation (2.2), and $\mu_i(\hat{S}_i)$ is the chemical potential of the atom species $\hat{S}_i$. Procedure (ii) - (iii) defines the MC step. In the multi-step MC equilibration process, each site is relaxed individually while all the other sites are held fixed. Each site change affects its four bond lengths, six bond angles and 12 angles of its nearest neighbours, thus, the energy change is calculated only for the above. This method is very efficient as was demonstrated by Weidmann and Newman [33]. It was also used by Glas [34].

The above defines our most general procedure D-(c) in which random 'flips' are considered for spins, atomic displacements and cell volumes. In our procedure D-(b) we avoid the *random* atomic and cell volume changes (i.e., steps (ii)a and (ii)c above) replacing this step by a deterministic *minimization* of E_{direct} with respect to $\{R_i\}$ and $\{\tau\}$, keeping the spin-configuration fixed. The minimization is done by a Monte Carlo equilibration process at temperature $T = 0$. Finally, in our simplest procedure D-(a) we freeze all atomic position and cell vectors of the ideal virtual lattice values and use pure *spin* flips (i.e., only step (ii)b above) in our MC procedure.

$Ga_{1-x}In_xP$ shows a phase-separating ground state, so the phase diagram exhibits a miscibility gap. The phase diagram of a phase-separating alloy $A_xB_{1-x}C$ can now be calculated as described by Kelires and Tersoff [6]. The compositions $x_1(T)$ and $x_2(T)$ of the two coexisting phases at a temperature T are obtained by plotting the composition $\langle x(\Delta\mu, T)\rangle$ averaged over the MC iterations versus $\Delta\mu = \mu_{AC} - \mu_{BC}$. The average $\langle x(\Delta\mu, T)\rangle$ exhibits a first order phase transition, where $x_1(T)$ and $x_2(T)$ are the coexisting compositions. Plotting $x_1(T)$ and $x_2(T)$ versus T gives the phase diagram.

The samples used in the present calculations consisted of periodically repeated cubic cells of $8 \times N \times N \times N$ atoms for $N = 5$. In order to accumulate enough statistics on the structural properties some 200 such samples with different spin configuration $\{\hat{S}_i\}$ were equilibrated for each case. We also checked for finite size effects by the calculation of selected points using our two basic algorithms, (i) internal energy minimization without any spin flips and (ii) MC equilibration process at $T > 0$ with spin flips. Using cubic cells of

$8 \times N \times N \times N$ atoms for $5 \leqslant N \leqslant 8$, we estimate that finite-size errors are below 1% for both algorithms.

3. Results

3.1. Effects of positional relaxation on the mixing enthalpy

The mixing enthalpy ΔH_{mix} is the excess enthalpy of the disordered alloy at (x, T) taken with respect to the energy of equivalent amounts of pure AC and BC at their equilibrium volumes

$$\Delta H_{\text{mix}}(x, T) = E(x, T) - [x E(\text{AC}) + (1 - x) E(\text{BC})] . \tag{11}$$

Figure 3 shows $\Delta H_{\text{mix}}(x, T = \infty)$ for the chemically perfectly random $\text{Ga}_{1-x}\text{In}_x\text{P}$ alloy neglecting vibrational effects. We give results with atomic relaxation $\Delta H_{\text{mix}}^{\text{r}}$ (dashed line), and without relaxation $\Delta H_{\text{mix}}^{\text{ur}}$ (solid line). Relaxation lowers ΔH_{mix} enormously: The *maximum value for the relaxed system* $\Delta H_{\text{mix}}^{\text{r}}(x = 0.47) = 77.1 \pm 0.1$ meV/four-atoms is much lower than the unrelaxed value $\Delta H_{\text{mix}}^{\text{ur}}(x = 0.53) = 152 \pm 1$ meV/four-atoms. The asterisks denote the formation enthalpies ΔH_F of few of the *ordered* structures, defined in table 1. The reduced enthalpy (interaction parameter) can be written as

$$\hat{\Omega}(x, T) = \Delta H(x, T)/x(1 - x). \tag{12}$$

If $\Delta H_{\text{mix}}(x)$ were parabolic, the interaction parameter $\hat{\Omega}(x)$ would be x independent. Fitting our $\Delta H_{\text{mix}}^{\text{r}}(x)$ to equation (12) shows, however a nearly linear behaviour $\hat{\Omega}(x) = \Omega_0 + ax$. Our fit to $\Delta H_{\text{mix}}^{\text{r}}(x)$ is

$$\hat{\Omega}(x, T = \infty) = 3.7 - 0.8x \ (\text{kcal mol}^{-1}) \tag{13}$$

showing that $\Delta H_{\text{mix}}(x)$ is not symmetric about $x = \frac{1}{2}$. Interestingly, for the relaxed alloy $a < 0$ while for the unrelaxed alloy $a > 0$ (compare the solid line to the dashed line in figure 3). Indeed $\lim_{x \to 0} \hat{\Omega}(x)$ and $\lim_{x \to 1} \hat{\Omega}(x)$ is the 'limiting solution enthalpy" representing the change in enthalpy when impurity amounts of A are added to BC. Our result thus indicates that for the *unrelaxed alloy*

$$\Delta H_{\text{mix}}^{\text{ur}}(\text{GaP} : \text{In}) < \Delta H_{\text{mix}}^{\text{ur}}(\text{InP} : \text{Ga}). \tag{14}$$

Thus, it costs *less* energy to dissolve a large atom (In) in a small host (GaP) than to dissolve a small atom (Ga) in a large host (InP). However, the opposite is true when relaxation is allowed, i.e.

$$\Delta H_{\text{mix}}^{\text{r}}(\text{GaP} : \text{In}) > \Delta H_{\text{mix}}^{\text{r}}(\text{InP} : \text{Ga}). \tag{15}$$

This result implies that the *effective* two-body force constant α_{eff} of the In–P bond within the GaP host is higher than that of the Ga–P bond within the InP host

$$\alpha_{\text{eff}}^{\text{In–P}}(\text{GaP}) > \alpha_{\text{eff}}^{\text{Ga–P}}(\text{InP}). \tag{16}$$

This is the reverse of the situation in the *pure binary* materials, where the VFF values are [28]

$$\alpha^{\text{In–P}}(\text{GaP}) < \alpha^{\text{Ga–P}}(\text{InP}). \tag{17}$$

3.2. Effects of configurational, positional and vibrational degrees of freedom on the phase diagram

Figure 4 shows the x–T phase diagram of the GaInP alloy calculated in our D-(c) approach. The circles connected by dashed lines denote the results of the MC calculations (interpolated near the top of the miscibility gap), while the squares denote the recent experimental results of Ishida *et al* [35]. The agreement is very reasonable, given that we fitted our interactions only to first-principle calculations on ordered superlattices. Table 3 gives the miscibility

Table 3. Different approximation to the upper miscibility temperature T_{MG} and composition x_{MG}, Mean-Field (MF) versus Monte Carlo (MC) . All approximations are based on the present interatomic T-VFF potential (see section 5.2).

Method	$\{R_i\}$	$\{\hat{S}_i\}$	ΔS_{vib}	$T_{MG}(K)$	x_{MG}
D-(a) (MF)	Unrelaxed	Random	Zero	1746	0.50
D-(b) (MF)	Relaxed	Random	Zero	833	0.50
D-(b) (MC)	Relaxed	Non-random	Zero	900 ± 40	0.42 ± 0.03
D-(c) (MC)	Relaxed	Non-random	Non-zero	870 ± 20	0.40 ± 0.02

gap (MG) temperature T_{MG} and composition x_{MG} for the various approximations D-(a), D-(b) and D-(c) explained schematically in figure 1. In addition, table 3 shows the effects of using a mean-field (MF), perfectly random spin variables instead of the correlated MC results. Note that when *perfectly* random alloys are considered, the (ideal) mixing entropy does not depend on the structure (but does depend on composition), so the equilibrium structure is decided by a positional relaxation without any spin flips. Thus, when perfectly random alloys are considered, δE of equation (2.10) is evaluated at a constant (random) spin configuration corresponding to a given composition x. This calculation resembles the process of quenching a sample which was initially equilibrated at some high temperature.

Table 3 shows the following features:

(i)   Comparison of approach D-(a) with D-(b), both executed using perfectly random (uncorrelated) spins shows how enormous is the effect of *positional relaxation* in these alloys: The miscibility gap temperature drops from 1746 K (unrelaxed random alloy) to 833 K (relaxed random alloy).

(ii)   Comparison of approach D-(b) executed within mean field theory to the same approach executed within Monte Carlo shows that *atomic (configurational) correlations* present in the latter *increase* the miscibility gap temperature by ~ 70 K. In this calculation we permit atomic correlations (i.e. short range order effects) in both ΔE and ΔS, while still neglecting vibrational effects. This is calculated by allowing in the MC runs spin-flips as well as complete atomic relaxations to the *lowest energy* of each spin configuration (this is distinguished from continuous-space MC where atoms are displaced along *random* directions which is not necessarily energy lowering). As usual, spin correlations tend to *reduce* the entropy relative to the mean field value. However, for phase-separating systems, spin correlation also made the enthalpy less positive [21]. Since $T_{MG} \propto \Delta H/\Delta S$, these correlation effects in ΔH and ΔS could have *opposite* influence on T_{MG}. We find that the net effect of atomic correlations is to increase the miscibility temperature.

(iii)   In the final step one introduces vibrational effects through the use of *random* displacements. Comparing approach D-(b) to D-(c) (both executed within the Monte Carlo approach) shows that *vibrational effects* lower T_{MG} to 870 ± 20 K and move x_{MG} to 0.40 ± 0.02.   The results of this calculation are shown in figure 4.   Thus, vibrations
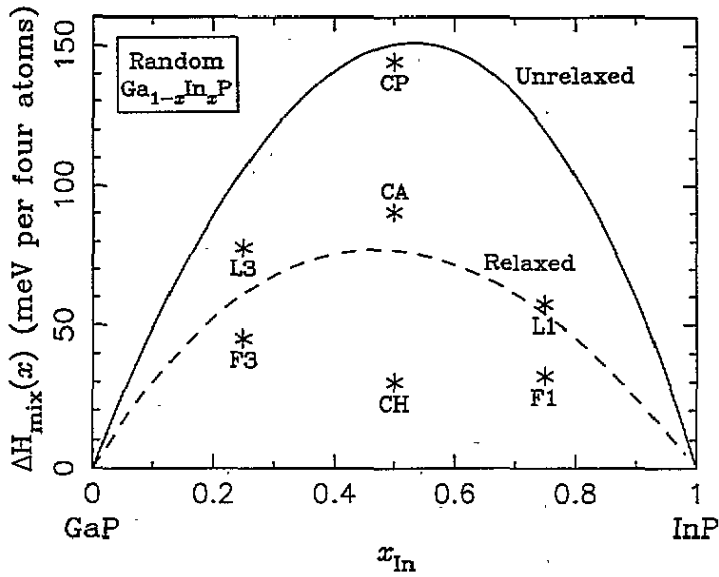
Figure 3. The mixing enthalpy of the chemically random $Ga_{1-x}In_xP$ alloy. The solid line denote the unrelaxed results while the dashed line denotes the relaxed mixing enthalpy. The asterisks denotes the formation enthalpy of some ordered structures $CP \approx CuPt$, $CA = CuAuI$, CH = chalcopyrite, F1, F3 = famatinite, and L1, L3 = luzonite. These structures are defined in [7] (figure 1 therein).
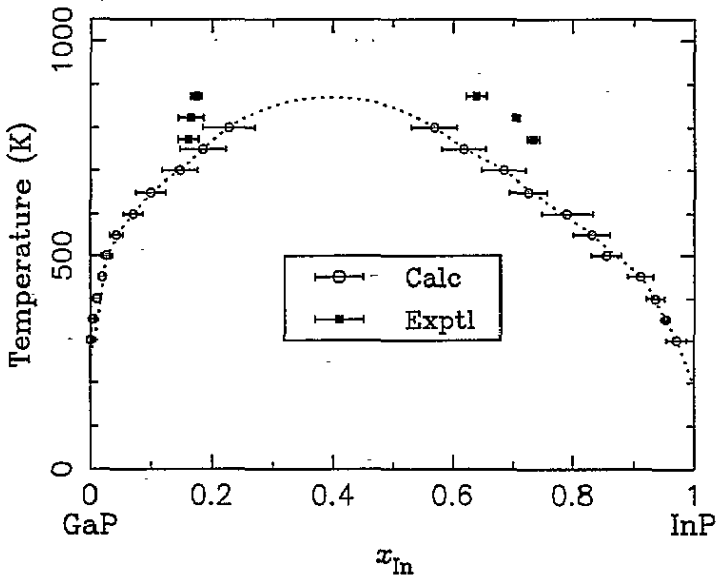

Figure 4. Calculated and measured $x-T$ phase diagram of the disordered $Ga_{1-x}In_xP$ alloy. The circles denote results of our Monte Carlo simulations, while the squares are experimental results of [35]. The dashed line is an interpolation of the calculated results.

tend to *lower* T_{MG}. The same trend was observed in empirical models that introduce vibrational effects into semiconductor alloy [36, 37] and noble metal alloy [38] phase diagrams. However, our *direct* calculation of vibrational effects suggests that previous *model* calculations [36, 37] may have overestimated the vibrational effects. For example, Garbulsky and Ceder [40] predict that the $x = \frac{1}{2}$ miscibility gap temperature of FCC lattices is affected by the chemical (J_{chem}) and vibrational (J_{vib}) nearest-neighbour effective cluster interactions as

$$T_{MG} \cong J_{chem} \frac{9.8}{1 + 9.8 J_{vib}}.$$ (18)

J_{vib} was estimated for 3D lattices as

$$J_{vib} \approx \frac{3}{8} \log \frac{K_{AA} K_{BB}}{K_{AB}^2}$$ (19)

where $K_{\alpha\beta}$ are ideal spring force constants for the $\alpha - \beta$ pair. Using the above, considering only nearest neighbour interactions in a 3D FCC binary alloy, and using a reasonable value of $K_{AA} K_{BB}/K_{AB}^2 = 1.3$ for the force constants, they estimated that vibrations lower T_{MG} by a factor of 2 from the value one would get neglecting the vibrations.

In the case of ternary tetrahedrally bonded semiconductors $A_{1-x}B_xC$ (like the $Ga_{1-x}In_xP$ alloy), each pair of cations A and B in the FCC sublattice are connected through an anion C. Therefore, the spring force constants of the mixed FCC sublattice are of a second neighbour interactions, and may be denoted as K_{A-C-A}, K_{B-C-B}, and K_{A-C-B}. The ratio $K_{A-C-A} K_{B-C-B}/K_{A-C-B}^2$ is much lower than the above ratio $K_{AA} K_{BB}/K_{AB}^2$, since for example K_{A-C-A} considers a connection through two A–C bonds while K_{A-C-B} considers a connection through one A–C bond and one B–C bond, so the difference between the K_{A-C-A} and K_{A-C-B} spring constants is much lower than the difference between the above FCC K_{AA} and K_{AB} spring constants which consider different kinds of bonds. Thus, the vibrational effective cluster interaction J_{vib}, calculated using equation (19) for ternary semiconductors will be much lower than J_{vib} for the case of FCC materials, therefore we predict that the vibrational lowering of T_{MG} for ternary semiconductors will not be so high as estimated by Garbulsky and Ceder [40] for FCC materials, but a minor effect.

4. Summary

Figure 1 explains the various approaches for calculating the thermodynamic properties of an alloy from its Born–Oppenheimer surface. While it would be interesting to check the extent to which various Ising cluster expansions mimic the original Born–Oppenheimer energy surface, we have concentrated here only on direct calculation methods that avoid Ising expansions. We find that for a size-mismatched phase-separating system (i) positional relaxations change significantly both ΔH_{mix} (from 152 to 77 meV/four atoms) and T_{MG} (from 1746 K to 833 K); (ii) atomic correlations (described via Monte Carlo) reduce both the entropy and the enthalpy. These competing effects on T_{MG} reflect in a net *increase* by 70 K; (iii) vibrational effects reduce T_{MG} further by 30 K and do not shift the critical composition.

Acknowledgments

References

[1] Zunger A 1994 *Nato Advanced Study Institute on Statics and Dynamics in Alloys* ed A Gonis and P Turchi (New York: Plenum) p 361
[2] Wolverton C, Lu Z W and Zunger A 1994 *Phys. Rev.* B **49** 16058
[3] Hohenberg P and Kohn W 1964 *Phys. Rev.* B **136** 864
   Kohn W and Sham L J 1965 *Phys. Rev.* A **140** 1133 Devreese J T and Van Camp P 1986 *Electronic Structure, Dynamics and Quantum Structural Properties of Condensed Matter* NATO series vol **121** (New York: Plenum)
[4] Catlow C R A and Mackrodt W C 1982 *Computer Simulations in Solids* (Berlin: Springer) Torrence I M 1972 *Interatomic Potentials* (New York: Academic)
[5] Foiles S M 1985 *Phys. Rev.* B **32** 7685
[6] Kelires P C and Tersoff J 1989 *Phys. Rev. Lett.* **63** 1164
[7] Wei S-H and Zunger A 1989 *Phys. Rev.* B **39** 3279
[8] Dünweg B and Landau D P 1993 *Phys. Rev.* B **48** 14182
[9] de Fontaine D 1979 *Solid State Physics* vol 34 ed H Ehrenreich, F Seitz and D Turnbull (New York: Academic) p 73
[10] Sanchez J M, Ducastelle F and Gratias D 1984 *Physica* A **128** 334
[11] Connolly J W D and Williams A R 1983 *Phys. Rev.* B **27** 5169
[12] Kanamori J and Yakehashi Y 1977 *J. Physique* **38** 274
   Ducastelle F 1991 *Order and Phase Stability in Alloys* (North Holland: Amsterdam)
[13] Kikuchi R 1974 *J. Chem. Phys.* **60** 1071; 1951 *Phys. Rev.* **81** 988
[14] Metropolis N, Rosenbluth A W, Rosenbluth M V, Teller A and Teller E 1953 *J. Chem. Phys.* **21** 1087
[15] Magri R, Bernard J E and Zunger A 1991 *Phys. Rev.* B **43** 1593
[16] Schmid F and Binder K 1995 in preparation
[17] Binder K 1986 *Festkörperprobleme (Advances in Solid State Physics)* vol 26 ed P Grosse (Vieweg: Braunschweig) p 133
[18] Lu Z W, Wei S-H and Zunger A 1991 *Phys. Rev. Lett.* **66** 1753
[19] Asta M, de Fontaine D, van Schilfgaarde M, Sluiter M and Methfessel M 1992 *Phys. Rev.* B **46** 5055
[20] Amador C, Lambrecht W R L, van Schilfgaarde M and Segall B 1993 *Phys. Rev.* B **47** 15276
[21] Wei S-H, Ferreira L G and Zunger A 1990 *Phys. Rev.* B **41** 8240
[22] Laks D B, Ferreira L G, Froyen S and Zunger A 1992 *Phys. Rev.* B **46** 12587
[23] de Gironcoli S, Giannozzi P and Baroni S 1991 *Phys. Rev. Lett.* **66** 2116
[24] Ferreira L G, Wei S-H and Zunger A 1989 *Phys. Rev.* B **40** 3197
[25] Dandrea R G, Bernard J E, Wei S-H and Zunger A 1990 *Phys. Rev. Lett.* **64** 36
   Mbaye A A, Ferreira L G and Zunger A 1987 *Phys. Rev. Lett.* **58** 49
   Wei S-H, Ferreira L G and Zunger A 1992 *Phys. Rev.* B **45** 2533
[26] Binder K and Reger J D 1992 *Advances in Physics* **41** 547
   Landau D P 1979 *Monte Carlo Methods in Statistical Physics* ed K Binder (Berlin: Springer) p 121-143
[27] Keating P N 1966 *Phys. Rev.* **145** 637
[28] Martins J L and Zunger A 1984 *Phys. Rev.* B **30** 6217
[29] Martin R M 1970 *Phys. Rev.* B **1** 4005
[30] Lu Z W, Laks D B, Wei S-H and Zunger A *Phys. Rev.* B at press
[31] Wei S-H and Krakauer 1985 *Phys. Rev. Lett.* **55** 1200
[32] Kirkpatrick S, Gelatt C D, Jr and Vecchi M P 1983 *Science* **220** number 4598 671
   Silverman A and Adler J 1992 *Computers in Physics* vol 6 No 3 277
[33] Weidmann M R and Newman K E 1992 *Phys. Rev.* B **45** 8388

[34] Glas F 1989 *J. Appl. Phys.* **66** 1667
[35] Ishida K, Nomura T, Tokunaga H, Ohtani H and Nishizawa T 1989 *J. Less-Common Met.* **155** 193
[36] Mohri T, Nakamura K and Ito T 1991 *J. Appl. Phys.* **70** 1320
[37] Nakamura K and Mohri T 1993 *Modelling Simul. Mater. Sci. Eng.* **1** 143
[38] Sanchez J M, Stern J P and Moruzzi V L 1991 *Phys. Rev.* B **44** 5411
[39] Sanchez J M, Garbulsky G D and Decer G 1994 *Phys. Rev.* B **49** 6327
[40] Garbulsky G D and Ceder G 1994 *Phys. Rev.* B. **49** 6327